Bioorganic Chemistry 89 (2019) 103040

Contents lists available at ScienceDirect

Bioorganic Chemistry

journal homepage: www.elsevier.com/locate/bioorg

An NIR emitting styryl dye with large Stokes shift to enable *co*-staining study on zebrafish neuromast hair cells

Lucas McDonald[a], Dipendra Dahal[a], Michael Konopka[a], Qin Liu[b,*], Yi Pang[a,*]

[a] Department of Chemistry, The University of Akron, Akron, OH 44325, United States
[b] Department of Biology, The University of Akron, Akron, OH 44325, United States

ARTICLE INFO

Keywords:
Neuromasts
Near Infrared (NIR) emission
Zebrafish
Styryl dye
Cyanine
Support cell
Excited state intramolecular proton transfer

ABSTRACT

Hearing loss is a significant public health problem, and the "loss of sensory hair cells" is one of two leading causes in humans. Advanced imaging reagents are desirable for understanding the role of the surrounding support cells in the loss or regeneration of the hair cells. A styryl dye was found to exhibit NIR emission ($\lambda_{em} \approx 684$ nm) with a very large Stokes shift ($\Delta\nu \approx 9190\ cm^{-1}$), due to the incorporation of excited state intramolecular proton transfer (ESIPT) mechanism. When used to stain live zebrafish embryos, the probe was found to exhibit good selectivity in targeting neuromasts, which are sensory organs on the surface of the fish's body. The finding was verified by direct comparison with the known neuromast-labeling reagent, 4-Di-2-ASP. In contrast to the existing styryl dyes that label neuromast hair cells, the new probe labeled *both* neuromast hair cells *and* the surrounding support cells, while giving discernable signals. The study thus illustrated a useful tool to aid the developmental study of two closely related cell types on the mechanosensory sensory organ of zebrafish, which is a powerful animal model for hearing loss research.

1. Introduction

As a model organism, zebrafish have been widely used in various biological studies [1,2]. They use a lateral line system to detect movement in surrounding water [3]. The lateral line is made up of mechanosensory organs called neuromasts that are distributed over the fish's head and body surface and is innervated by the lateral line nerves (Fig. 1) [1,3,4]. Because hair cells in the lateral line are functionally similar to hair cells in the inner ear of mammals, the zebrafish neuromast has been adopted as a model for studying hair cell regeneration [5–7]. The neuromast model study could shed light on the hearing-loss problems, as "loss of hair cells" is one of two leading causes for hearing loss in humans [8,9]. Due to its clinical relevance, the zebrafish lateral line has emerged as a powerful animal model for screening drugs that cause or prevent hair cell death [10]. Broad interests in advancing hair cell research are described in recent review articles [11,12].

The lateral line comprises of a series of individual neuromasts that are composed of sensory hair cells and surrounding support cells. The support cells include two distinct cell populations: (i) inner support cells under the hair cells, and (ii) mantle cells that encircle the entire neuromasts (Fig. 1) [5,13]. The available tools for recognition of neuromasts include transgenic methods and use of vital fluorescent dyes [5,7]. Although few transgenic fish lines have been generated for labeling specific cell types within neuromasts [5], it is often difficult to distinguish the two major cell types (i.e., hair cells and surrounding support cells). It is not known if support cells are a homogeneous population, or if only subsets of support cells contribute to regeneration [5]. In order to gain a better understanding of the developmental process of hair cells, it is important to visualize simultaneously both hair cells and their surrounding support cells.

Among the available tools for imaging the lateral lines, vital dyes are arguably the easiest and most accessible reagents used to visualize the lateral hair cells [7]. Scheme 1 lists the structures of the commonly used vital dyes, which include a styryl pyridinium segment and exhibit emission between 590 and 610 nm. As a common feature, this class of dyes exhibits good selectivity in labeling neuromasts of zebrafish lateral lines. The mechanism of labeling has been examined by using FM1-43 [14]. The styryl dyes can quickly label hair cells by entering through open mechanotransduction channels.

Although styryl dyes have been widely used to stain zebrafish for neuromast imaging, there are some drawbacks that need to be improved. First, the staining is often incomplete; *Neuromasts that are not labeled by styryl dyes such as DASPEI are not always completely devoid of hair cells*, as observed in the study of Rubel et al. [15]. Second, the intensity of staining begins to fade within several minutes after washing out the dye, since neuromast staining (by styryl dyes such as DASPEI) is

* Corresponding authors at: University of Akron, Akron, OH 44325, USA.
E-mail addresses: qliu@uakron.edu (Q. Liu), yp5@uakron.edu (Y. Pang).

https://doi.org/10.1016/j.bioorg.2019.103040
Received 14 January 2019; Received in revised form 29 May 2019; Accepted 3 June 2019
Available online 03 June 2019
0045-2068/

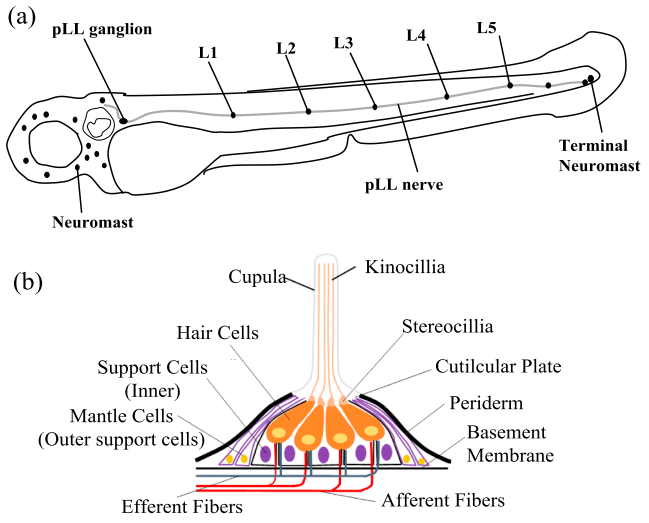

Fig. 1. (a) Sketch of the lateral line sensory organ on a zebrafish at 72 hpf. (b) The structure of an enlarged neuromast.

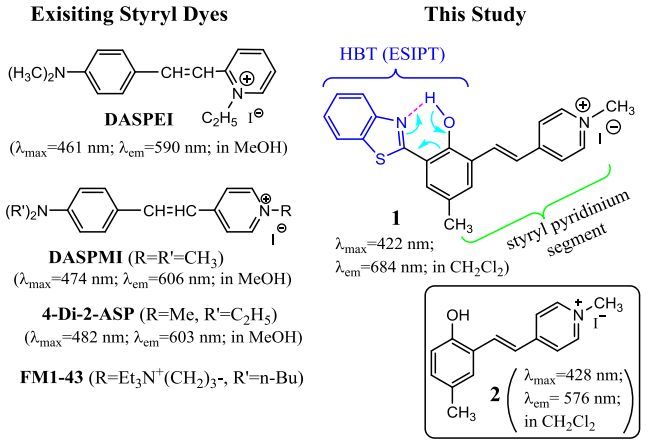

Scheme 1. Structures of commercial styryl dyes and compound **1**, along with their absorption and fluorescence.

limited to endoplates on superficial fibers [16]. Despite these drawbacks that make it difficult for quantitative comparison, styryl dyes (e.g. DASPEI and 4-Di-2-ASP) are still commonly used for imaging of neuromasts [1,7,17]. A previous study showed that 4-Di-2-ASP was more effective than DASPEI in staining nerve terminals [16], and is widely used for labeling the neuromast [7,18–21]. It should be noted that no existing fluorescent dyes are known to label the support cells, which is essential for correlation between the hair cells and related support cells. Therefore, it is desirable to develop new probes that can display the support cells to advance the neuromast study.

Excited state intramolecular proton transfer (ESIPT) has emerged to be an attractive mechanism for the design of fluorescent molecular probes, due to its ability to generate large Stokes shift in emission signals [22]. For example, ESIPT-based chemosensors have been used for detecting zinc cation [23,24] and various anions. Our recent study shows that coupling an ESIPT unit with a cyanine fragment could drastically improve the fluorophore's Stokes shift and fluorescence quantum yields [25]. The concept of developing cyanine-containing ESIPT fluorophores is further examined by synthesis of probe **1**, whose structure includes a benzothiazole group for ESIPT at the hydrophobic end of styryl dyes. Interestingly, probe **1** exhibits excellent selectivity for plasma membrane of prokaryotic (*E. coli*) cells [26]. In this contribution, we demonstrate that probe **1** also shows selective interactions with neuromast cells, as it includes a styryl pyridinium segment. The study thus leads to the discovery of an attractive neuromast labeling reagent, which can reveal not only the neuromast hair cells, but also their surrounding support cells. Herein we report the optical characteristics of **1** and its potential use for neuromast labeling, in comparison with the commercial styryl dye 4-Di-2-ASP.

2. Results and discussion

Compound **1** was synthesized as reported recently from our laboratory [25,26]. Probe **1** exhibited emission at λ_{em} = 697 nm with a large Stokes shift ($\Delta\lambda \approx 292$ nm), which was slightly affected by solvent polarity (Fig. 2b). In sharp contrast, the emission wavelength of the typical styryl dye 4-Di-2-ASP (λ_{em} = 562 nm, $\Delta\lambda \approx 25$ nm) in CH_2Cl_2 was quite different from that in water (λ_{em} = 618 nm, $\Delta\lambda \approx 137$ nm) (Fig. 2a).

A unique structural feature in **1** is that the benzothiazole and pyridinium vinyl substituents are connected via a 1,3-phenylene bridge. As a consequence, the effective chromophore of **1** can be approximated by "chromophore I" (Scheme 2), due to effective π-conjugation interruption at the 1,3-phenylene bridge [28]. However, formation of the excited *keto* tautomer **3a** extended the conjugation of the styryl pyridinium segment as indicated by "chromophore II," resulting in a large bathochromic shift in emission. Therefore, the large Stokes shift from the fluorescence of **1** could be attributed to the effective formation of the *keto* tautomer **3a** that was only available in the excited state. Since ESIPT is a fast process (~150 fs) [27], only emission from its *keto* form **3a** was observed (Scheme 2), giving only one emission at ~680 nm. It

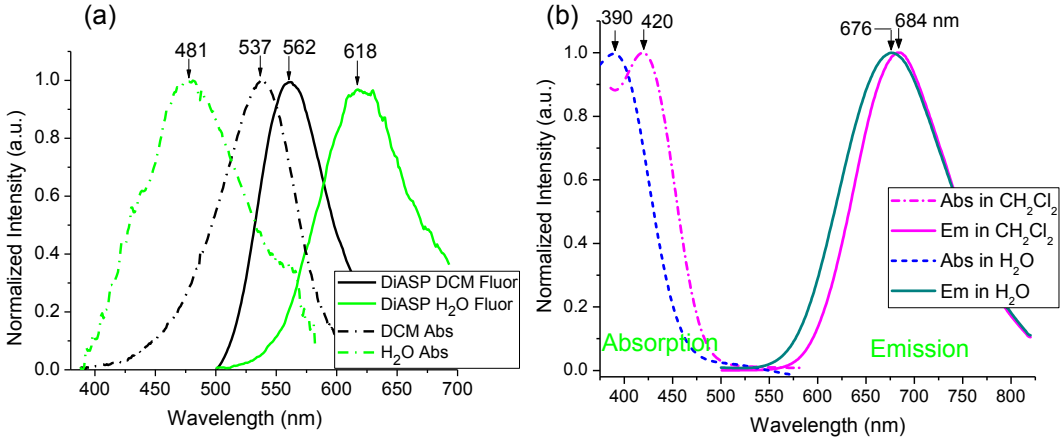

Fig. 2. Normalized UV–vis absorption (broken lines) and fluorescence (solid lines) spectra of 4-Di-2-ASP (a) and **1** (b) in CH_2Cl_2 and H_2O (10 μM solution) at 20 °C. Excitation for **1** at 390 and 420 nm.

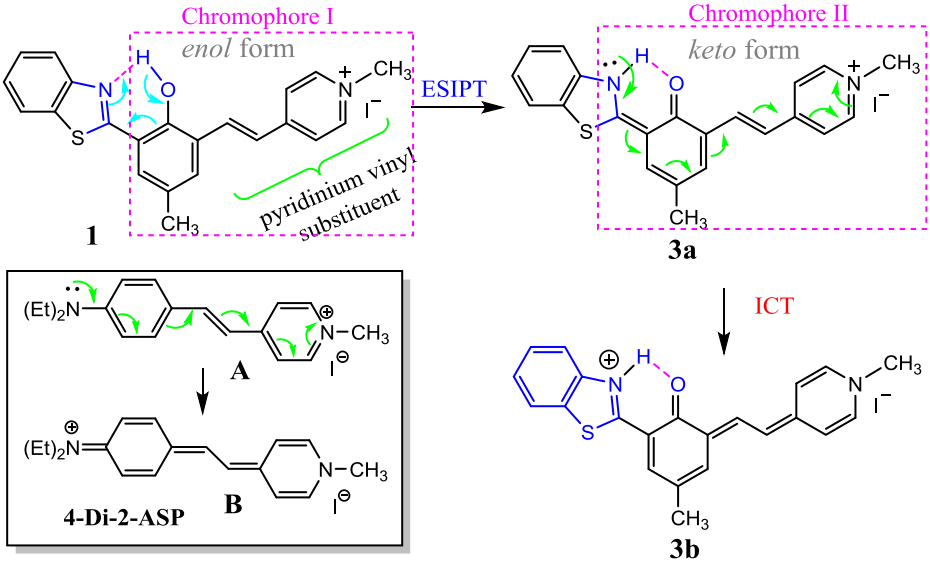

Scheme 2. Schematic illustration of formation of the *keto* form via excited state intramolecular proton transfer (ESIPT). And the intramolecular charge transfer.

should be noted that the observed emission $\lambda_{em} \approx 680$ nm was not due to the possible formation of phenoxide (Ar—OH → Ar—O^-), as the phenolic proton in **1** is not acidic ($pK_a = 8.26$) and the resulting phenoxide would be non-fluorescent [26].

Comparison of photophysical properties revealed that fluorescence quantum yield ϕ_{fl} of **1** was ~5 times higher than that of the styryl dye (Table 1), which is desirable for imaging applications. In order to shed some light on the fluorescence enhancement, we examined the photophysical characteristics of hemicyanine **2**. It should be noted that compound **2** can be considered as the effective chromophore of **1**, due to the efficient conjugation interruption at 1,3-phenylene bridge [28]. While the ϕ_{fl} of **2** was comparable to that of 4-Di-2-ASP, it was significantly lower than that of **1** (Table 1). The results pointed to that inclusion of the ESIPT unit in **1** could enhance the fluorescence of styryl dyes, as the intramolecular hydrogen bonding in **1** increases the molecular rigidity. The observed higher ϕ_{fl} from **1** could be partially attributed to the *meta*-phenylene bridge in the molecular design, which is known as "*meta effect*" to enhance the fluorescence [29,30].

In a wide range of solvents examined, the absorption λ_{abs} of **1** was less affected by solvents (except in CH_2Cl_2), in comparison with the model compound **2** and 4-Di-2-ASP (Fig. 3a, Table 1). A likely reason was that the fast ESIPT quickly transformed the excited **1** to its *keto* form **3a** (Scheme 2), which minimized the impact of solvent relaxation on the excited **1**. The solvent polarity also exhibited less impact on the emission λ_{em} of **1**, in comparison with **2** and 4-Di-2-ASP (Fig. 3b). As a consequence, the emission λ_{em} of **1** exhibited only a small spectral shift ($\Delta\lambda_{em} \sim 8$ nm, bathochromic shift) from H_2O to CH_2Cl_2 solvent (Fig. 2), in sharp contrast to that from the styryl dye 4-Di-2-ASP ($\Delta\lambda_{em} \sim 56$ nm, hypsochromic shift). Since interaction with biological cells typically involves movement of dye molecules from H_2O to a non-aqueous environment (e.g. lipid bilayers or proteins), negligible spectral shift in the emission will provide a more reliable signal for study.

Structural similarity of **1** to styryl dyes such as 4-Di-2-ASP, in terms of containing pyridinium vinyl substituent, encouraged us to seek its potential applications in biological systems. When applied to developing zebrafish, probe **1** showed selective labeling of neuromasts in the embryos (Fig. 4). The labeling pattern by using **1** (Fig. 4a & c) was comparable to that using 4-Di-2-ASP (Fig. 4b & d), a recognized neuromasts marker [16,19]. In the experiments, all embryos (< 72 h post fertilization, hpf) were removed from their chorions before staining to allow consistent staining. The 4-Di-2-ASP staining of the fish neuromasts was carried out as described by Magrassi et al (50 μM for 1 h) [16]. Zebrafish staining by probe **1** was accomplished with 10 μM for 30 min before washing with E3 medium 3 times. The experiments were repeated three times, all showing consistent results.

Although **1** was used in a lower concentration (10 μM), its fluorescence was comparable with the observed intensity of 4-Di-2-ASP (50 μM) labeling (Fig. 4). Non-neuromast labeling was observed from both probes (mainly in the yolk) in 72 hpf embryos (Fig. 4c and d), while the neuromast labeling (indicated by the arrowheads) was easily distinguishable from the background labeling in the low magnification images. Comparison between the neuromast labeling patterns in the head region of these embryos revealed that probe **1** labeled neuromasts were larger than those labeled with 4-Di-2-ASP (Fig. 4e and f).

Higher magnifications of one of the head neuromasts showed that there were fewer labeled neuromast cells using 4-Di-2-ASP than using probe **1** (Fig. 4g & h). It appeared that both probes labeled cells in the central region of the neuromasts (likely hair cells), while probe **1** also weakly labeled most peripherally located cells (mainly cell membranes; likely support cells). The observed larger neuromasts in the probe **1**

Table 1
Photophysical Properties of **1** and 2-Di-4-ASP in DCM at 20 °C.

Compound	In H_2O		In DCM	
	Absorption	Fluorescence	Absorption	Fluorescence
1	$\lambda_{abs} = 390$ nm; ($\varepsilon = 2.83 \times 10^4$)	$\lambda_{em} = 676$ nm $\phi_{fl} = 0.06$	$\lambda_{abs} = 420$ nm; ($\varepsilon = 2.92 \times 10^4$)	$\lambda_{em} = 684$ nm $\phi_{fl} = 0.34$
2-Di-4-DSP	$\lambda_{abs} = 481$ nm;	$\lambda_{em} = 618$ nm $\phi_{fl} = 0.0066$	$\lambda_{abs} = 537$ nm;	$\lambda_{em} = 562$ nm $\phi_{fl} = 0.0785$
2	$\lambda_{abs} = 380$ nm; ($\varepsilon = 1.03 \times 10^4$)	$\lambda_{em} = 587$ nm $\phi_{fl} = 0.003$	$\lambda_{abs} = 428$ nm; ($\varepsilon = 9.1 \times 10^3$) $LM^{-1}\,cm^{-1}$	$\lambda_{em} = 576$ nm $\phi_{fl} = 0.076$

Note: molar absorption coefficient ε is calculated at absorption maximum.

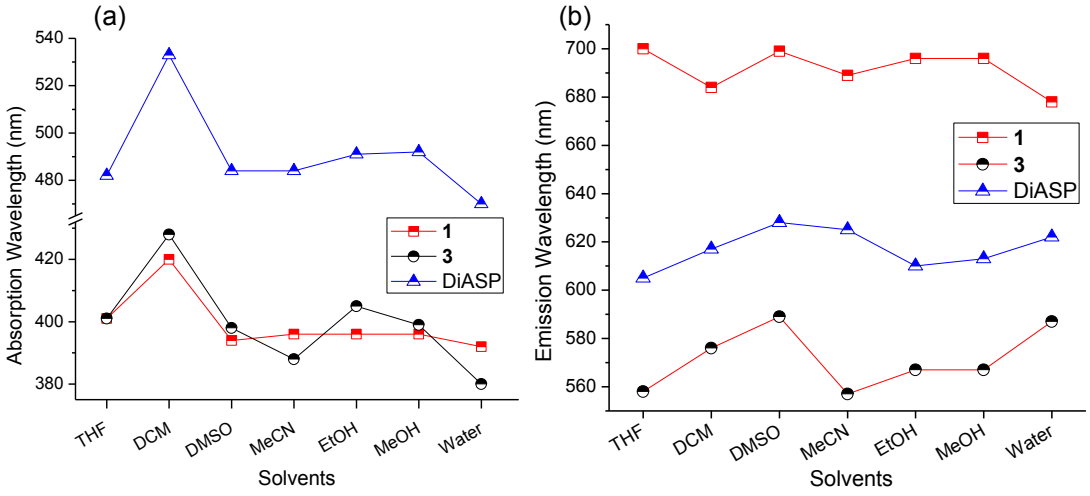

Fig. 3. UV–vis absorption λ_{abs} (a) and fluorescence λ_{em} (b) of **1**, **2** and 4-Di-2-ASP in different solvents. All data were collected at 20 °C.

labeling was thus attributed to its ability to label *not only* the hair cells, *but also* the surrounding support cells. Interestingly, the difference in probe **1** labeling intensities of these cells was such that two different cell populations (i.e. strongly labeled central cells, and weakly stained peripheral cells) could be readily discerned (Fig. 4h). The results indicated that probe **1** was a more selective and stronger marker for the neuromasts in developing zebrafish. Furthermore, application of probe **1** required use of lower concentration and shorter time for neuromast labeling (in comparison with 4-Di-2-ASP), benefitting from its NIR emission that is not interfered by autofluorescence.

On the basis of the observed bright emission (Fig. 4F), it was assumed that the probe **1** quickly labeled neuromast hair cells, due to the strong interaction of styryl pyridinium segment. Further penetration of probe **1** would bring the probe molecules to the support cells immediately underneath the hair cells (i.e. inner support cells). Thus, use of probe **1** exhibited a distinct advantage: labeling both the hair and support cells, while being able to differentiate them. To the best of our knowledge, probe **1** was the first styryl dye to exhibit such a property. In the molecular design, the styryl pyridinium segment of **1** was responsible for the hair cell selectivity. The HBT segment at the hydrophobic end of **1** was *not only* enabling ESIPT, *but also* providing some desired function for membrane staining. The probe's ability to give discernable signals for the hair and support cells thus provided a possible staining method for studying the development of hair cells in relation to the surrounding support cells, which remains to be a challenge in the hair cell research [31,32].

3. Regeneration of neuromast cells by co-staining

Different from the existing neuromast labeling (e.g. 4-Di-2-ASP), probe **1** exhibited a transparent window, with no absorption and emission between 500 and 575 nm (see Fig. 2b). Since the absorption

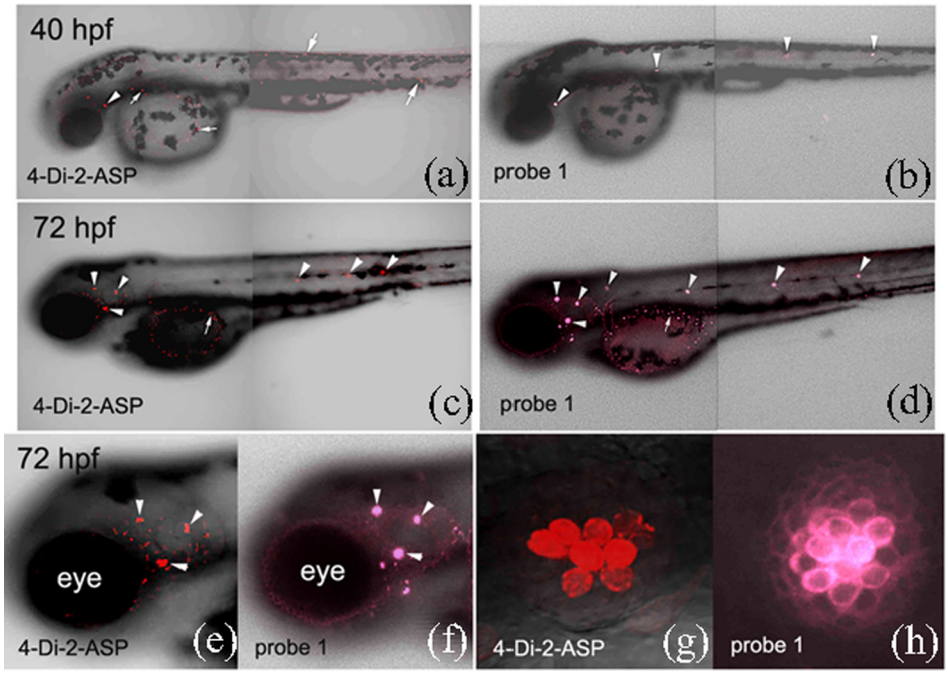

Fig. 4. Confocal images of zebrafish embryos (40–72 hpf) labeled with 4-Di-2-ASP or probe **1**. Anterior to the left and dorsal up for all images. Excitation wavelength was at 488 nm with a 595 nm filter (Texas Red) for 4-Di-2-ASP, and at 405 nm with filters at 700 nm (Texas Red and Cy5) for probe **1**, respectively. Neuromasts and non-neuromasts labeling was indicated by arrowheads and arrows, respectively.

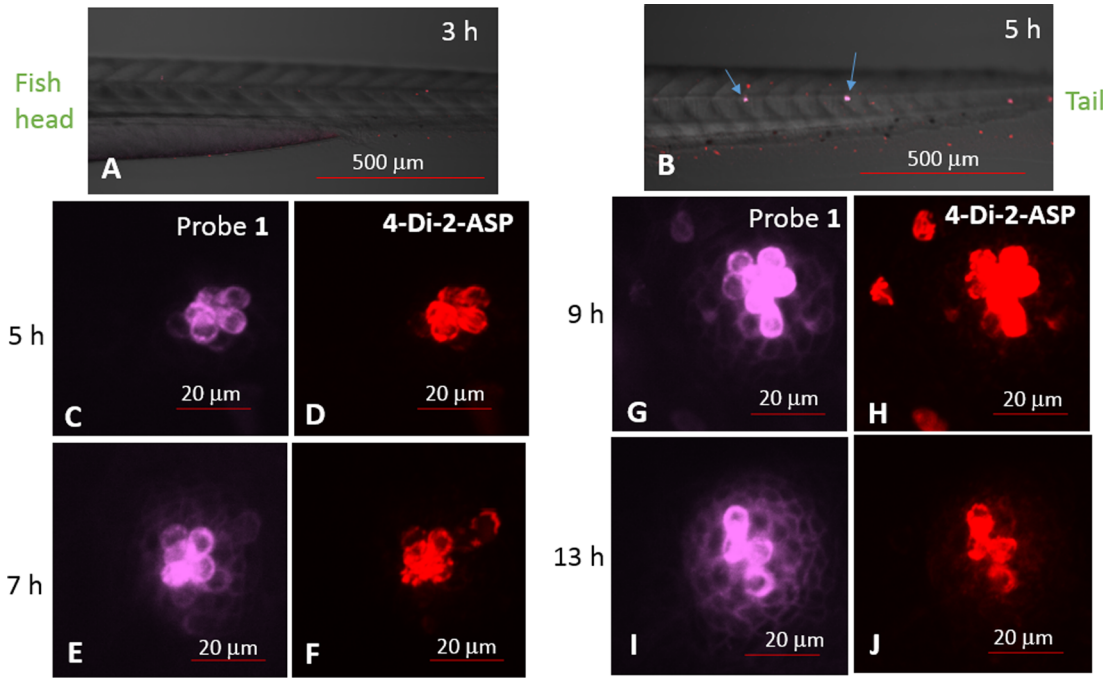

Fig. 5. Confocal images of neuromasts from a live zebrafish, 3, 5, 7, 9 and 13 h after initial treatment with 250 µM neomycin for 1 h. Panels A & B are posterior halves of zebrafish larvae (anterior to the left, dorsal up), where arrows indicate labeled neuromasts. Panels C, E, G and K are high magnification images viewed from probe **1** (λ_{ex} at 405 nm); panels D, F, H and L are from 4-Di-2-ASP (λ_{ex} at 488 nm).

($\lambda_{max} \approx 537$ nm) and emission ($\lambda_{em} \approx 562$ nm) of 4-Di-2-ASP in non-aqueous environment (e.g. CH_2Cl_2) is within the optical window, it opens the possibility of simultaneous imaging of hair and support cells in a biological event. Due to the large Stokes shift, the emission of **1** has no overlap with the absorption of 4-Di-2-ASP, thereby eliminating the energy transfer between the dyes used for *co*-staining. In order to further demonstrate the unique advantage of **1**, we decided to monitor the developmental process of hair cells during their regeneration, which is related to the hearing loss research. Thus 80 hpf zebrafish larvae were treated with neomycin-containing medium (neomycin concn 250 µM) for 1 h by using a known procedure [15], which effectively killed almost all hair cells.

Three hours following the neomycin treatment, the larvae were co-stained with probe **1** and 4-Di-2-ASP (10 µM for each) for 30 min and washed again with E3 media before imaging, no hair cells were labeled (Fig. 5A). At 5 h post treatment (hpt), labeled hair cells started to be detected, which were observed from both **1** and 4-Di-2-ASP labeling (Fig. 5B, C & D), but the support cells were not labeled. At 7 hpt, the support cells became faintly labeled with **1**, but not with 4-Di-2-ASP labeling (Fig. 5E–F). From 9 to 13 hpt, more support cells were detected as shown with **1** labeling (Fig. 5G, I). Based on these results, it appeared that the neuromast regeneration started from hair cells, which was followed by support cell regeneration. This is different from what is known about the sequence of neuromast regeneration (i.e. hair cell regeneration depend on support cells) [5,32]. It is possible that inner support cells (those situated directly below the hair cells) survived the neomycin treatment, but were masked by the above and much more intensely labeled hair cells. These inner support cells may play a role in the hair cell regeneration. The co-staining experiment consistently displayed that probe **1** was more selective in labeling hair cells, as 4-Di-2-ASP exhibited a higher tendency to label other cells (in addition to the hair cells) (see Fig. 5H).

In the co-staining experiment, the region of support cells were clearly defined. In the early stage (5 hpt, Fig. 5C), the surrounding support cells were not observed. At 7 hpt (Fig. 5E), the hair cells were only increased slightly, while the support cells were observed. From 7 to 9 hpt (Fig. 5E & G), the surrounding support cells were not uniformly distributed. Failure to observe the surrounding support cells at the beginning stage of regeneration (Fig. 5C) suggests that the inner support cells played more significant roles during the initial stage of hair cell regeneration.

4. Conclusion

Incorporation of a styryl pyridinium group led to the development of probe **1** that gave NIR emission and exhibited excited state intramolecular proton transfer (ESIPT). Optical comparison between **1** and a styryl dye (4-Di-2-ASP) revealed that the emission of **1** exhibited a higher fluorescence quantum efficiency (Table 1) with a very large Stokes shift ($\Delta\nu \approx 9190\ cm^{-1}$). In addition, the emission of **1** was less affected by different solvent environments, in sharp contrast to the styryl dye whose absorbance and emission were more sensitive to different environments. These properties make probe **1** an attractive candidate for imaging applications.

When applied to zebrafishes, probe **1** was found to stain the fish's neuromasts selectively, giving bright imaging. Direct comparison with the neuromast labeling reagent 4-Di-2-ASP showed that probe **1** labeling exhibited improved selectivity to neuromast. Remarkably, probe **1** *not only* labeled neuromast hair cells, *but also* the adjacent support cells, in contrast to the existing neuromast labeling reagents that only label the hair cells. Since probe **1** exhibited a transparent optical window (i.e. no absorption and emission between 500 and 550 nm), it could be used for co-staining with other compatible imaging reagents. For the first time, via co-staining with 4-Di-2-ASP, the study illustrated a useful imaging method that can simultaneously reveal the activities of both support cells and hair cells, whose correlation are important in neuromast development. Since support cells play important roles in the development, function, and regeneration of neuromast hair cells [30], the developed probe could aid the study of hair cell regeneration and discovery of the related drugs. We anticipate the use of the developed probe could assist the researchers to pursue the following fundamental questions in the fields [5]: (a) could support cells be a homogeneous population? and (b) could specific subset of support cells play more significant roles for hair cell regeneration?

5. Experimental section

5.1. General considerations

All reactions were carried out under aerobic conditions. All reagents were purchased through VWR, DMSO and 4-Di-2-ASP was purchased form Sigma, and ethanol was purchased from Decon Laboratories. All materials were used as received without further purification. All ^{1}H and ^{13}C data were collected using Varian 300 and 500 MHz instruments with all spectra referenced to deuterated solvents.

5.2. Synthesis of (E)-4-(3-(benzo[d]thiazol-2-yl)-2-hydroxy-5-methylstyryl)-1-methylpyridin-1-ium **(1)**

3-(benzo[*d*]thiazol-2-yl)-2-hydroxy-5-methyl- benzaldehyde (0.548 g) was added to a solution of 4-methylpicoline (0.470 g) in methanol. Piperidine (0.5 mL) was added to the mixture and it was refluxed overnight before removing solvent via rotory evaporation. The resulting solid was washed with ethyl acetate and filtered before washing with water and completely drying under high vacuum yielding a dark purple solid (65% yield). Mp 208–210 °C. ^{1}H NMR (DMSO-d_6, 300 MHz) $\delta = 8.73$ (d, $J = 8.73$, 2H, Ar—H), 8.19–8.06 (m, 4H), 8.02 (d, $J = 7.8$ Hz, 1H, Ar—H), 7.9 (s, 1H, Ar—H), 7.74 (d, $J = 16.2$ Hz, 1H, alkene), 7.61 (s, 1H, Ar—H), 7.53 (t, $J = 7.9$ Hz, 1H, Ar—H), 7.43 (t, $J = 7.4$ Hz, 1H, Ar-H), 4.19 (s, 3H, $-CH_3$), 2.33 (s, 3H, $-CH_3$). ^{13}C NMR (DMSO-d_6, 125 MHz) δ 167.69, 153.92, 151.58, 144.94, 137.84, 134.10, 133.45, 131.33, 126.84, 125.23, 124.32, 123.11, 122.46, 122.15, 121.89, 119.33, 47.01, 20.52. ESI-MASS *m/z* calcd for $[C_{25}H_{21}N_2O_2S]^+$: 413.1324; found: 413.1324.

5.3. Zebrafish breeding

Zebrafish (*Danio rerio*) were maintained as described in the Zebrafish Book [33]. They were kept in 10-gallon tanks with 28.5 °C water and 12 h light/12 h dark cycle. Zebrafish embryos were obtained by breeding adult wildtype. Zebrafish embryos were obtained by breeding adult wildtype zebrafish. All embryos were maintained in E3 medium (15 mM NaCl, 0.5 mM KCl, 1 mM $MgSO_4$, 1 mM $CaCl_2$, 0.15 mM KH_2PO_4, 0.05 mM Na_2HPO_4, 0.7 mM $NaHCO_3$, and 10^{-5}% methylene blue at 7.5 pH) at 28.5 °C. All animal related procedures were approved by the Care and Use of Animals in Research Committee at The University of Akron.

5.4. Zebrafish staining and imaging

The stock solution of **1** or 4-Di-2-ASP (1 mM concentration) was prepared in DMSO. All fish embryos were removed from their chorions before staining. Embryos of 24, 36, 48, 60, and 72 h post fertilization (hpf) were uded in this study. At each stage of development, the embryos from the same breeding were stained with either styryl dye 4-Di-2-ASP (50 μM for 1 h) or probe **1** (10 μM for 30 min), before washing with E3 medium 3 times. Imaging was performed on a Nikon A1 confocal system with a Plan Apo λ 10x and a Plan Fluor 40x Oil DIC H N2 objectives with both GaAsP detectors and high sensitivity low noise PMTs for detection. Excitation wavelength for DiApi was 488 nm with a 595 nm filter (Texas Red) and excitation for **1** was 405 nm with filters at 595 and 700 nm (Texas Red and Cy5 respectively). Images were processed using NIS Elements software.

6. Disclosure

Dr. Michael Konopka provided access and use of a fluorescent confocal microscope along with any assistance in data capture that was required. Dr. Qin Liu bread and harvested all zebrafish embryos and provided analysis of staining patterns and assisted in developmental description and analysis of the embryos'. Dipendra Dahal synthesized and characterized the cyanine dye (probe **1**). Lucas McDonald helped in characterization of the dye, stained and treated all embryos, performed all imaging studies with guidance from Dr. Liu and Dr. Pang for experimental design. Dr. Yi Pang was the principal investigator for this project and assisted in all characterization and experimental design.

Acknowledgment

We thank support from NIH (Grant no. 1R15GM126438-01A1). Y.P. also acknowledges partial support from Coleman Endowment from The University of Akron.

Data availability

Authors confirm that the data supporting the findings of the study are available within the article.

References

[1] M. Froehlicher, A. Liedtke, K.J. Groh, S.C.F. Neuhauss, H. Segner, R.I.L. Eggen, Zebrafish (Danio rerio) neuromast: promising biological endpoint linking developmental and toxicological studies, Aquat. Toxicol. 95 (4) (2009) 307–319.
[2] A. Nechiporuk, D.W. Raible, FGF-dependent mechanosensory organ patterning in zebrafish, Science 320 (5884) (2008) 1774.
[3] A. Ghysen, C. Dambly-Chaudiere, Development of the zebrafish lateral line, Curr. Opin. Neurobiol. 14 (1) (2004) 67–73.
[4] A.B. Chitnis, D.D. Nogare, M. Matsuda, Building the posterior lateral line system in zebrafish, Dev. Neurobiol. 72 (3) (2012) 234–255.
[5] M.E. Lush, T. Piotrowski, Sensory hair cell regeneration in the zebrafish lateral line, Dev. Dyn. 243 (10) (2014) 1187–1202.
[6] T. Nicolson, The genetics of hearing and balance in zebrafish, Annu. Rev. Genet. 39 (2005) 9–22.
[7] A.B. Coffin, H. Brignull, D.W. Raible, E.W. Rubel, Hearing loss, protection, and regeneration in the larval zebrafish lateral line, in: S. Coombs, H. Bleckmann, R.R. Fay, A.N. Popper (Eds.), The Lateral Line System, Springer, New York, 2014, pp. 313–347.
[8] Based on the data from Hearing Loss Association of American, about 20% Americans (48 million) report some degree of hearing loss. At age 65, one out of three people has a hearing loss. http://www.hearingloss.org/content/basic-facts-about-hearing-loss (accessed December 2017).
[9] More than 90 percent of hearing loss occurs when either hair cells or auditory nerve cells are destroyed. See NIH fact sheets: Hair Cell Regeneration and Hearing Loss. https://report.nih.gov/nihfactsheets/viewfactsheet.aspx?csid=94 (accessed December 2017).
[10] H.C. Ou, F. Santos, D.W. Raible, J.A. Simon, E.W. Rubel, Drug screening for hearing loss: using the zebrafish lateral line to screen for drugs that prevent and cause hearing loss, Drug Discov. Today 15 (2010) 265–271.
[11] A.B. Coffin, J. Ramcharitar, Chemical ototoxicity of the fish inner ear and lateral line, in: J. Sisneros (Ed.), Fish Hearing and Bioacoustics, 2016, pp. 419–437.
[12] J.S. Kniss, L. Jiang, T. Piotrowski, Insights into sensory hair cell regeneration from the zebrafish lateral line, Curr. Opin. Genet. Dev. 40 (2016) 32–40.
[13] E.Y. Ma, D.W. Raible, Signaling pathways regulating zebrafish lateral line development, Curr. Biol. 19 (9) (2009) R381–R386.
[14] J.R. Meyers, R.B. MacDonald, A. Duggan, D. Lenzi, D.G. Standaert, J.T. Corwin, Lighting up the senses: FM1-43 loading of sensory cells through nonselective ion channels, J. Neurosci. 23 (2003) 4054–4065.
[15] J.A. Harris, A.G. Cheng, L.L. Cunningham, G. MacDonald, D.W. Raible, E.W. Rubel, Neomycin-induced hair cell death and rapid regeneration in the lateral line of zebrafish (*Danio rerio*), J. Assoc. Res. Otolaryngol. 4 (2) (2003) 219–234.
[16] L. Magrassi, D. Purves, J.W. Lichtman, Fluorescent probes that stain living nerve terminals, J. Neurosci. 7 (4) (1987) 1207–1214.
[17] M. Haehnel, M. Taguchi, J.C. Liao, Heterogeneity and dynamics of lateral line afferent innervation during development in zebrafish (*Danio rerio*), J. Comp. Neurol. 520 (7) (2012) 1376–1386.
[18] D. Alexandre, A. Ghysen, Somatotopy of the lateral line projection in larval zebrafish, Proc. Natl. Acad. Sci. USA 96 (13) (1999) 7558–7562.
[19] W.K. Metcalfe, Sensory neuron growth cones comigrate with posterior lateral line primordial cells in zebrafish, J. Comparat. Neurol. 238 (1985) 218–224.
[20] P.P. Hernandez, V. Moreno, F.A. Olivari, M.L. Allende, Sub-lethal concentrations of waterborne copper are toxic to lateral line neuromasts in zebrafish (*Danio rerio*), Hear. Res. 213 (2006) 1–10.
[21] E.J. Villablanca, A. Renucci, D. Sapède, V. Lec, F. Soubiran, P.C. Sandoval, C. Dambly-Chaudière, A. Ghysen, M.L. Allende, Control of cell migration in the zebrafish lateral line: implication of the gene "Tumour-Associated Calcium Signal Transducer," *tacstd*, Dev. Dyn. 235 (6) (2006) 1578–1588.
[22] S.J. Formosinho, L.G. Arnaut, Excited-state proton transfer reactions II. Intramolecular reactions, J. Photochem. Photobiol. A. Chem. 75 (1993) 21–48.
[23] M. Taki, J.L. Wolford, T.V. O'Halloran, Emission ratiometric imaging of intracellular zinc: design of a benzoxazole fluorescent sensor and its application in two-photon microscopy, J. Am. Chem. Soc. 126 (3) (2004) 712–713.
[24] Y. Xu, Q. Liu, B. Dou, B. Wright, J. Wang, Y. Pang, Zn2+ binding-enabled excited

state intramolecular proton transfer: a step toward new near-infrared fluorescent probes for imaging applications, Adv. Healthcare Mater. 1 (4) (2012) 485–492.
[25] D. Dahal, L. McDonald, X. Bi, C. Abeywickrama, F. Gombedza, M. Konopka, S. Paruchuri, Y. Pang, An NIR-emitting lysosome-targeting probe with large Stokes shift via coupling cyanine and excited-state intramolecular proton transfer, Chem. Commun. 53 (2017) 3697–3700.
[26] D. Dahal, K.R. Ojha, N. Alexander, M. Konopka, Y. Pang, An NIR-emitting ESIPT dye with large stokes shift for plasma membrane of prokaryotic (*E. coli*) cells, Sens. Actuat. B Chem. 259 (2018) 44–49.
[27] C.C. Hsieh, Y.M. Cheng, C.J. Hsu, K.Y. Chen, P.T. Chou, Spectroscopy and femtosecond dynamics of excited-state proton transfer induced charge transfer reaction, J. Phys. Chem. A 112 (36) (2008) 8323–8332.
[28] Q. Chu, Y. Pang, L. Ding, F.E. Karasz, Green-emitting PPE-PPV hybrid polymers: efficient energy transfer across the m-phenylene bridge, Macromolecules 36 (11) (2003) 3848–3853.
[29] F.D. Lewis, J.S. Yang, The excited state behavior of aminostilbenes. A new example of the meta effect, J. Am. Chem. Soc. 119 (1997) 3834–3835.
[30] Y. Pang, J. Li, B. Hu, F.E. Karasz, A highly luminescent poly[(m-phenylenevinylene)-alt-(p-phenylenevinylene)] with defined conjugation length and improved solubility, Macromolecules 32 (1999) 3946–3950.
[31] D.W. Raible, G.J. Kruse, Organization of the lateral line system in embryonic zebrafish, J. Comp. Neurol. 421 (2000) 189–198.
[32] E.L. Monzack, L.L. Cunningham, Lead roles for supporting actors: Critical functions of inner ear supporting cells, Hear. Res. 303 (2013) 20–29.
[33] M. Westerfield, The Zebrafish Book. A Guide for the Laboratory Use of Zebrafish (*Danio rerio*), fourth ed., Univ. of Oregon Press, Eugene, 2000.